Title

Numerical Evaluation of Nitrate Distributions in the Onion Root Zone under Conventional Furrow Fertigation

Journal

Journal of Hydrologic Engineering, 21(2)

ISSN

1084-0699

Authors

Deb, Sanjit K
Sharma, Parmodh
Shukla, Manoj K
et al.

Publication Date

2016-02-01

DOI

10.1061/(asce)he.1943-5584.0001304

Peer reviewed

Numerical Evaluation of Nitrate Distributions in the Onion Root Zone under Conventional Furrow Fertigation

Sanjit K. Deb[1]; Parmodh Sharma[2]; Manoj K. Shukla[3]; Jamshid Ashigh[4]; and Jiří Šimůnek[5]

Abstract: HYDRUS (2D/3D) model was used to simulate spatial and temporal distributions of nitrate-nitrogen (NO_3-N) within and below the onion root zone under conventional furrow fertigation with the urea-ammonium-nitrate (UAN) liquid fertilizer. The simulated water contents in the furrow irrigated onion field agreed well with the measurements. Simulations produced similar patterns of the measured NO_3-N concentration profiles throughout the growing season. NO_3-N concentrations remained higher and accumulation of NO_3-N was observed within the root zone. Higher NO_3-N within the root zone was dependent on the rate of the UAN fertilizer application, quantity of NO_3-N removed by root uptake, and NO_3-N drainage fluxes below the root zone. Simulations also suggested that NO_3-N below the root zone during different growth stages remained much higher than a recommended (for drinking water) standard concentration level (10 mg L^{-1}). This resulted in higher NO_3-N drainage fluxes, particularly during the fertigation events between the establishment and vegetative growth stages. This indicates the need to apply most fertigation events at an early stage of bulb formation to provide the maximum NO_3-N demands by onions and to reduce potential NO_3-N leaching. **DOI: 10.1061/(ASCE)HE.1943-5584.0001304.** © *2015 American Society of Civil Engineers.*

Author keywords: Furrow irrigation; Fertigation; Nitrate leaching; *HYDRUS (2D/3D)* model; Onion; Simulation.

Introduction

Of all the essential nutrients, nitrogen (N) is required by crops in the largest quantity and is most frequently the limiting factor in crop productivity. From various sources of N losses in irrigated agriculture that decrease the availability of N to crops, leaching is considered a major source of nitrate (NO_3^-) loss (Sharma et al. 2012a, b). Apart from the economic considerations of nutrient losses, fertilization practices in irrigated agriculture directly and indirectly affect the composition of groundwater recharge and aquifer biogeochemistry (Böhlke 2002). The highly soluble complex ion NO_3^-, which is only weakly adsorbed by particles in most soils, is a common contaminant of groundwater (Spalding and Exner 1993; González–Delgado and Shukla 2014). Groundwater contamination by NO_3^- leaching continues to be of great agroenvironmental concern in climatic regions where irrigated agriculture is dominating and excessive N fertilizers are applied to arable soils every year.

In addition to soil properties, N fertilizers, and water applied by irrigation or received through precipitation, a type of irrigation system also plays an important role in NO_3^- leaching to groundwater (Al-Jamal et al. 1997; Sharma et al. 2012a, b). The problem of NO_3^- leaching can be exacerbated in agricultural areas, such as in the arid and semiarid southern New Mexico, where surface or flood irrigation systems are widely practiced on highly permeable coarse textured soils. Irrigation systems such as sprinkler or drip to alleviate NO_3^- leaching require large initial capital expenditures when converting from low energy furrow irrigation. Furrow irrigation remains the commonly used method in arid and semiarid regions of the world to irrigate vegetables and row crops, and in particular, the specialty crop onion (*Allium cepa*) in southern New Mexico. New Mexico produces onions primarily for the fresh market, and on average, onions are New Mexico's most profitable crop. During the 2011 to 2013 seasons, New Mexico supplied 28–31% of summer, nonstorage onions consumed in the United States (USDA 2014). Approximately 2,400 ha of onions were planted, and 2,350 hectares were harvested annually (2011–2013), producing approximately 138,840 t at a value of $47 million (USDA 2014).

NO_3^- leaching is a common problem in frequently fertilized agricultural crops in southern New Mexico. Accumulation or distribution of NO_3^- in the crop root zone and its leaching vary considerably with crops (Weed and Kanwar 1996; Al-Jamal et al. 1997; Sharma et al. 2012b) because crops differ in rooting depths, rooting densities, N and water requirements, and crop uptake efficiencies (Peterson and Power 1991). Al-Jamal et al. (1997) reported that NO_3^- loadings to groundwater were greater for onion than for chile pepper (*Capsicum annuum*) in the furrow irrigation systems in southern New Mexico. In another study, NO_3^- loadings below the root zone under furrow irrigation systems were found to be the highest for onion, followed by chile pepper and cotton (*Gossypium* spp.) (Sharma et al. 2012b).

Direct measurements of simultaneous water flow and NO_3^- accumulation within or losses below the crop root zone are not only laborious, time-consuming, and expensive, but also highly challenging, primarily because of uncertainties associated with estimating drainage fluxes and solute concentrations in the leachate, even under well-controlled experimental conditions

[1]Assistant Professor, Dept. of Plant and Soil Science, Texas Tech Univ., P.O. Box 42122, Lubbock, TX 79409; formerly, Postdoctoral Fellow, Dept. of Plant and Environmental Sciences, New Mexico State Univ., MSC 3Q, P.O. Box 30003, Las Cruces, NM 88003 (corresponding author). E-mail: sanjit@nmsu.edu; sanjit.deb@ttu.edu

[2]Statistical Programmer, PVR Technologies, King of Prussia, PA 19406; formerly, Graduate Research Assistant, Dept. of Plant and Environmental Sciences, New Mexico State Univ., Las Cruces, NM 88003.

[3]Professor, Dept. of Plant and Environmental Sciences, New Mexico State Univ., Las Cruces, NM 88003.

[4]Field Scientist, DOW AgroSciences Canada Inc., London, ON N6H4Z8; formerly, Associate Professor, Dept. of Extension Plant Sciences, New Mexico State Univ., Las Cruces, NM 88003.

[5]Professor, Dept. of Environmental Sciences, Univ. of California, Riverside, CA 92521.

Note. This manuscript was submitted on November 2, 2014; approved on August 14, 2015; published online on October 14, 2015. Discussion period open until March 14, 2016; separate discussions must be submitted for individual papers. This paper is part of the ***Journal of Hydrologic Engineering***, © ASCE, ISSN 1084-0699.

(van der Laan et al. 2010). Simulation models have become valuable research tools for predicting complex and interactive processes of water flow and solute transport in and below the root zone. Models are useful for identifying potential environmental risks associated with leaching of surface-applied fertilizers, such as with furrow fertigation, the process of applying soluble fertilizers [e.g., liquid N fertilizer consisting of a mixture of urea, ammonium (NH_4^+), and nitrate (NO_3^-)] along with irrigation. Yet, few computer simulation models, with the exception of *HYDRUS (2D/3D)* (Šimůnek et al. 2012), have the capability to analyze water flow and nutrient transport in multiple spatial dimensions. The *HYDRUS* model has been extensively used for simulating water flow and solute transport in a variety of soil geometries, irrigation systems, and fertigation strategies for different crops [e.g., Cote et al. (2003), Gärdenäs et al. (2005), Hanson et al. (2006), Crevoisier et al. (2008), and Siyal et al. (2012)]. Notably, *HYDRUS (2D/3D)* has also proven to be an effective tool in improving our understanding of the soil-plant-atmosphere water relations in irrigated orchards of southern New Mexico (Deb et al. 2013).

A previous field study by Sharma et al. (2012a) has generated considerable information on nitrate-nitrogen (NO_3-N) leaching [i.e., $0.2259 \times NO_3^-$ (mg L^{-1})] from an onion field under conventional furrow fertigation in southern New Mexico. Numerical simulations of two-dimensional water flow and urea-ammonium-nitrate reactions and transport in the onion root zone, while accounting for root water and nutrient uptake by onion, can further improve our understanding of the dynamic nature of these processes under furrow fertigation. The scarcity of quantitative information on simultaneous water flow and NO_3-N movement and distribution within and below the crop root zone under furrow fertigation is equally true for the frequently fertilized onion. Therefore, the main objective of this study was to use the *HYDRUS (2D/3D)* model to simulate spatial and temporal distributions of NO_3-N within and below the onion root zone under furrow fertigation. *HYDRUS (2D/3D)* could provide an additional tool for examining NO_3-N distributions in the furrow irrigated onion production system.

Materials and Methods

Field Description

The study was carried out on a conventional furrow irrigated onion (*Allium cepa*) field at New Mexico State University's Leyendecker Plant Science Research Center (PSRC) in Las Cruces, New Mexico (32° 11.46′ N, 106° 44.40′ W and 1,128 m above mean sea level). Soil at the study site is classified as Glendale (fine-silty, mixed, calcareous, thermic typic Torrifluvents) and Harkey (coarse-silty, mixed, calcareous, thermic typic Torrifluvents). The study region is arid, with an average air temperature of 17.7°C and annual precipitation of 29.7 cm (Gile et al. 1981). The field was under onion–sudan (*Sorghum sudanense*) grass rotation for several years. Onion was transplanted on November 1, 2006 and harvested on July 14, 2007 [corresponds to 255 DAT (days after transplanting)]. Approximately 3–4 weeks before transplanting, the field was prepared following the conventional tillage practices, including disking followed by chiseling. Triple superphosphate was broadcasted at a rate of 200 kg P_2O_5 ha^{-1} on the field before plowing. The entire field was plowed to the depth of 20 cm to incorporate sudan grass stubble into the top soil layer, and then leveled using laser leveling technique. A lister was used to make furrows. Following the commonly used practice in southern New Mexico, onions were transplanted in two rows on each ridge.

Table 1. Dates of Fertigation Events in the Furrow Irrigated Onion Field during the Growing Season

Number of application	Irrigation/ fertigation date	Days after transplanting (DAT)	N application rate[a] (kg N ha^{-1})
1	November 5, 2006	4	12.3
2	November 17, 2006	16	—
3	November 29, 2006	28	12.3
4	December 15, 2006	44	—
5	January 8, 2007	68	—
6	February 9, 2007	100	49.2
7	February 23, 2007	114	—
8	March 6, 2007	125	49.2
9	March 16, 2007	135	—
10	March 27, 2007	146	49.2
11	April 5, 2007	155	—
12	April 13, 2007	163	49.2
13	April 20, 2007	170	—
14	April 27, 2007	177	49.2
15	May 12, 2007	192	24.6
16	May 25, 2007	205	—
17	June 1, 2007	212	—
18	June 7, 2007	218	12.3
19	June 15, 2007	226	—
20	June 21, 2007	232	12.3
21	June 29, 2007	240	—

[a]Fertilized with the urea-ammonium-nitrate (UAN) liquid fertilizer.

Onions were irrigated 21 times (Table 1) during the growing season. The water table was located at a depth greater than 2 m from the soil surface (Deb et al. 2011), and the field was irrigated with groundwater. The amount of water applied during each irrigation event was measured with a flow meter (McCrometer, Hemet, California). Staff gauges were installed in the furrow to continuously measure the depth of irrigation water during an irrigation event. On average, water application rate of 7500 L h^{-1} $furrow^{-1}$ for a 210 m long row was used, and water supply was stopped when the furrow was filled to about half the ridge height. Onions were fertilized with the urea-ammonium-nitrate (UAN) liquid fertilizer (32–0–0) (Table 1). Furrow fertigation was applied at a rate of 12.3 kg N ha^{-1} per irrigation during the establishment stage of onion growth (1 to 90 DAT), 49.2 kg N ha^{-1} per irrigation during the development (vegetative) and early stage of bulb formation (91 to 166 DAT), and 24.6 to 49.2 kg N ha^{-1} per irrigation during the bulb formation or bulb growth stage (167 to 207 DAT), and 12.3 kg N ha^{-1} per irrigation during the bulb enlargement or maturity stage (208 to 255 DAT).

Numerical Modeling

HYDRUS (2D/3D) Software

The two–dimensional water flow and NO_3^- dynamics were simulated using the finite element model *HYDRUS (2D/3D)*, version 2.03.450 (hereinafter referred to as *HYDRUS*) (Šimůnek et al. 2012). Detailed descriptions of the governing equations for water flow and solute transport and of the interactive graphical, Windows-based user interface can be found in the *HYDRUS (2D/3D)* technical (Šimůnek et al. 2012) and user manuals (Šejna et al. 2013), respectively. *HYDRUS* numerically solves the Richards' equation, which describes the isothermal Darcian water flow in a variably-saturated, rigid, isotropic porous medium and can be expressed as follows:

$$\frac{\partial \theta}{\partial t} = \nabla(K \nabla H) - S_r \tag{1}$$

where θ = volumetric water content ($cm^3\,cm^{-3}$); K = unsaturated hydraulic conductivity ($cm\,d^{-1}$); H = hydraulic head (cm); S_r = a sink term that represents the volume of water removed from a unit volume of soil per unit time attributable to plant water uptake ($cm^3\,cm^{-3}\,d^{-1}$); ∇ = spatial gradient operator; and t = time (d). Soil hydraulic properties (i.e., unsaturated retention and hydraulic conductivity functions) in Eq. (1) were described using the van Genuchten–Mualem functional relationships (van Genuchten 1980; Mualem 1976) as follows:

$$\theta(\psi) = \begin{cases} \theta_r + \dfrac{\theta_s - \theta_r}{[1 + (|\alpha_v \psi|^n)]^m} & \psi < 0 \\ \theta_s & \psi \geq 0 \end{cases} \tag{2}$$

$$K(\psi) = K_s S_e^l [1 - (1 - S_e^{1/m})^m]^2 \tag{3}$$

where θ_s = saturated volumetric water contents ($cm^3\,cm^{-3}$); θ_r = residual volumetric water contents ($cm^3\,cm^{-3}$); ψ = soil water pressure head; α_v = reciprocal of the air–entry $\psi(cm^{-1})$; $m = 1 - 1/n (n > 1)$; n = pore-size distribution index (unitless); S_e = effective saturation (unitless) given as $S_e = [\theta(\psi) - \theta_r]/(\theta_s - \theta_r)$; l = pore-connectivity parameter (unitless); and K_s = saturated hydraulic conductivity ($cm\,d^{-1}$). The sink term (S_r) without the osmotic stress was described according to the root water uptake model of Feddes et al. (1978), as implemented in the *HYDRUS*.

HYDRUS allows simultaneous simulation of multiple solutes that can be either independent of each other or subject to the first-order degradation reactions (e.g., N species). The solute transport equation considers advective-dispersive transport in the liquid phase, and diffusion in the gaseous phase. Urea, NH_4^+, and NO_3^- were considered for the N species simulations. The governing solute transport equations, which describe the transport of each N species, namely, urea, NH_4^+, and NO_3^-, can be written as follows:

$$\frac{\partial \theta c_1}{\partial t} = \nabla(\theta D \nabla c_1) - \nabla(q c_1) - \mu_a \theta c_1 - S_r c_1 \tag{4}$$

$$\frac{\partial \theta c_2}{\partial t} + \rho \frac{\partial s_2}{\partial t} = \nabla(\theta D \nabla c_2) - \nabla(q c_2) - \mu_v \theta c_2 - \mu_n \theta c_2 + \mu_a \theta c_1 - S_r c_2 \tag{5}$$

$$\frac{\partial \theta c_3}{\partial t} = \nabla(\theta D \nabla c_3) - \nabla(q c_3) + \mu_n \theta c_2 - S_r c_3 \tag{6}$$

where c_1, c_2, and c_3 = liquid phase concentrations ($mg\,cm^{-3}$) of urea, NH_4^+, and NO_3^-, respectively; D = dispersion coefficient tensor ($cm^2\,d^{-1}$); q = volumetric flux density ($cm\,d^{-1}$); ρ = bulk density of the soil ($g\,cm^{-3}$); s_2 = adsorbed concentration of NH_4^+ ($g\,g^{-1}$); μ_a = first-order rate constant (d^{-1}) representing nitrification of urea to NH_4^+; μ_v = first-order rate constant (d^{-1}) representing volatilization of NH_4^+ to ammonia (NH_3); and μ_n = first-order reaction rate constant (d^{-1}) representing nitrification of NH_4^+ to NO_3^-. Note that volatilization of NH_4^+ and subsequent NH_4^+ transport by gaseous diffusion was neglected in this study.

Urea and NO_3^- were assumed to be present only in the dissolved phase [i.e., the distribution coefficient $(K_d) = 0\ cm^3\ g^{-1}$]. The relationship between NH_4^+ in the solution (c_2) and NH_4^+ absorbed (s_2) is described by means of a linear adsorption isotherm as follows:

$$s_2 = K_d c_2 \tag{7}$$

NH_4^+ was assumed to adsorb to the solid phase and a K_d value of $3.5\ cm^3\ g^{-1}$ was used based on similar values reported in several studies [e.g., Ling and El-Kadi (1998) and Hanson et al. (2006)]. Eqs. (4)–(6) are linear as the reaction rate constants μ_a, μ_v, and μ_n, and the distribution coefficient for $NH_4^+(K_d)$ are concentration independent. The μ_a acts as a sink in Eq. (4) and as a source in Eq. (5). Similarly, the μ_n acts as a sink in Eq. (5) and as a source in Eq. (6). Molecular diffusion was neglected because it was considered negligible relative to hydrodynamic dispersion. The longitudinal dispersivity was considered equal to one-tenth of the profile depth (i.e., 11 cm) and the transverse dispersivity equal to one–tenth of the longitudinal dispersivity (i.e., 1.1 cm) (Beven et al. 1993; Cote et al. 2003; Hanson et al. 2006). Because of the lack of experimental data, the parameters μ_a and μ_n were also taken from the literature. The value was found to be between 0.02 and 0.72 for μ_a and between 0.36 and 0.56 for μ_n in the literature (e.g., Hanson et al. 2006). As suggested by Hanson et al. (2006) in their simulations with *HYDRUS–2D*, the μ_a and μ_n especially for fertigation with the UAN fertilizer were taken as 0.38 and 0.2 d^{-1}, respectively.

The last term in Eqs. (4)–(6) represents the passive root nutrient uptake, i.e., the movement of nutrients into roots by convective mass flow of water, which is directly coupled with root water uptake (Šimůnek and Hopmans 2009), and therefore, the products of root water uptake (S_r) and concentrations of respective species (i.e., c_1, c_2, and c_3, respectively). Because unlimited passive nutrient uptake for N species was considered, the maximum concentration of the root solute uptake was set to a concentration value larger than the dissolved simulated concentrations (c_1, c_2, and c_3), which allowed all dissolved nutrients to be taken up by plant roots with root water uptake.

Numerical Flow Domain and Its Spatial Discretization

The flow domain, 102 cm wide and 110 cm deep from the ridge, considered for simulating water flow and transport of N species (i.e., urea, NH_4^+, and NO_3^-) in the root zone of a furrow irrigation system is shown in Fig. 1. The width of the flow domain (102 cm) represents two halves of a 46 cm furrow [including both the bottoms (lengths AB and EF) and sloping sides (lengths BC and DE)] and a complete 56 cm ridge (length CD) at the upper boundary (Fig. 1). The finite element mesh was generated using the *MESHGEN* module of *HYDRUS*. The finite element mesh was refined such that the size of the elements was smaller near the soil surface along the ridge and two halves of the furrow where infiltration and evaporation, i.e., changes in the soil water content and corresponding pressure heads, were most rapid. The size of the elements was larger along the left and right boundaries (lengths AH and FG, respectively; Fig. 1), and the bottom boundary (length GH; Fig. 1) of the flow domain. The numbers of finite element nodes, boundary 1D-elements, and 2D-elements (triangles) in the flow domain were 8,282, 344, and 16,218, respectively. Observation nodes were located below the bottom of the furrow at soil depths of 20 and 50 cm from the ridge, which corresponded to the measurement locations of soil water contents during the onion growing season.

Initial and Boundary Conditions

The ridge surface (length CD; Fig. 1) was specified as an atmospheric boundary, defined by potential evaporation, potential transpiration, and rainfall. Both the bottom surfaces (AB and EF; Fig. 1) and sloping sides (BC and DE) of the furrow were assigned time-variable head boundary conditions, which were adjusted dynamically depending upon the water level (i.e., saturation

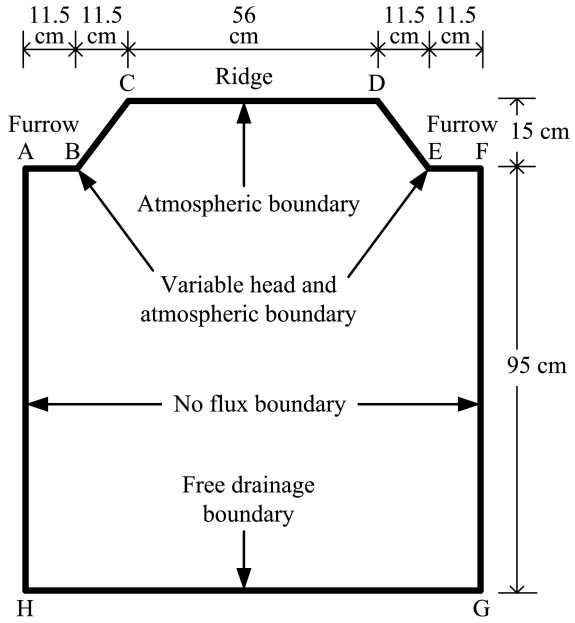

Fig. 1. Schematic of the flow domain with boundary conditions used in *HYDRUS (2D/3D)* simulations

conditions) in the furrow and conditions in the flow domain (i.e., the root zone). These boundaries switched from time-variable head boundary conditions to atmospheric boundary conditions when the pressure head (ψ) across these boundaries became negative (i.e., unsaturated conditions). In *HYDRUS*, the actual evaporation remains equal to the potential evaporation (E_p) as long as ψ at the atmospheric boundary is higher than a critical pressure head ψ_{crit} (considered to be −15,000 cm in this study). Once the ψ_{crit} value is reached, i.e., the soil surface dries out to the ψ_{crit} value, the actual evaporation rate is decreased from the E_p value. In the study areas, the water table was deep (>2 m from the soil surface), and did not affect flow in the transport domain of interest. Therefore, the bottom of the flow domain (GH; Fig. 1) was assigned a free drainage (i.e., a unit hydraulic gradient) boundary condition for gravitational flow to occur from the bottom of the 110 cm well-drained soil profile. Because of symmetry, the nodes representing the left and right boundaries (AH and FG, respectively; Fig. 1) of the flow domain were set as no-flux boundaries because no flow or solute transport occurred across these boundaries.

The initial distribution of the volumetric water contents (θ) at the day of transplanting (November 1, 2006) was based on gravimetrically measured values in the furrows at six soil depths (0–10, 10–30, 30–40, 40–60, 60–85, and 85–110 cm from the ridge). The initial θ distribution varied from 0.17 at the ridge to 0.22 $cm^3\,cm^{-3}$ at the bottom of the 110-cm soil profile. Because sudan grass was not fertilized, the flow domain was considered N free at the beginning of the simulation, and the initial concentrations of urea, NH_4^+, and NO_3^- were thus assumed to be zero. The urea, NH_4^+, and NO_3^- fluxes out of the flow domain could occur only from the bottom free drainage boundary. The cumulative leaching of mass of each N species (urea, NH_4^+, and NO_3^-) out of the bottom boundary was controlled by the concentration of each N species at that depth and the corresponding water flux density as computed from Eq. (1). A third-type (Cauchy) boundary condition was specified at the time-variable head, atmospheric, and free drainage water flow boundary conditions. The Cauchy boundary condition defined the concentration flux of each N species (urea, NH_4^+, and NO_3^-) across the boundary.

Field Measurements and Model Input Requirements

The characterization of the soil profile (0–110 cm soil depths) at this onion field were reported in Deb et al. (2011) and Sharma et al. (2012a). Briefly, the soil texture is sandy loam down to 80 cm soil depth and sand below 80 cm. Therefore, the 110 cm flow domain was assumed to be a homogeneous, with a bulk density varying from 1.3 to 1.5 mg m^{-3} (average = 1.4 mg m^{-3}). The value of K_s ranged from 49 to 107 cm d^{-1} within the 110 cm soil profile, with an average value of 50 cm d^{-1}. The average soil pH and electrical conductivity (EC) for the 0–60 cm depths were 7.4 and 2.0 dS m^{-1} and were 8.0 and 0.8 dS m^{-1} for depths greater than 60 cm, respectively. On average, within the 0–60 cm depths, soil organic matter, phosphorus (P), and potassium (K) were 0.43%, 11.6 mg L^{-1}, and 57.3 mg L^{-1}, and at soil depths > 60 cm, were 0.02%, 2.2 mg L^{-1}, and 29 mg L^{-1}, respectively.

The soil water retention curve was determined using the pressure chamber method at ψ of 0 (at saturation), −300, −500, −1,000, −3,000, −5,000, −10,000, and −15,000 cm H_2O. The values of θ_s (= 0.43 $cm^3\,cm^{-3}$), θ_r (= 0.07 $cm^3\,cm^{-3}$), α_v (= 0.003 cm^{-1}), and n (= 2.03) were estimated by fitting the van Genuchten (1980) soil water retention model to the measured drainage curve data using the *RETC* code (van Genuchten et al. 1991). The value of the parameter l was assumed to be 0.55 (Deb et al. 2011). Temporal variations in volumetric water contents (θ) in the soil profile at a location below the bottom of a furrow at soil depths of 20 and 50 cm from the ridge were measured using a set of two time domain reflectometry (TDR) sensors (CS640) (Campbell Scientific, Logan, Utah). A total of eight TDR sensors were installed at four field locations below the bottom of the furrows to record the volumetric soil water content every 10 min during the onion growing season.

Irrigation water samples were collected during each month and analyzed for EC, pH, NO_3-N, and chloride. Bulk soil samples were collected monthly from the furrows at six soil depths down to 110 cm from the ridge. The gravimetric water content was determined for each bulk soil sample. Bulk soil samples were air dried for 48 h, grounded, and passed through a 2-mm diameter sieve. A Technicon Autoanalyzer II (Technicon Instruments, Tarrytown, New York) with the cadmium reduction column technique was used to analyze soil-KCl extracts for NO_3-N (Maynard and Kalra 1993).

HYDRUS requires as time-variable inputs separate values of potential evaporation (E_p) from the soil surface and potential transpiration (T_p) through the plants. Meteorological variables were obtained from the PSRC weather station, which included precipitation, solar radiation, air and soil surface temperatures, wind speed, and relative humidity measured on an hourly basis at 2 m above the soil surface. The daily reference evapotranspiration for grass (ET_0) was estimated based on the FAO–56 Penman–Monteith equation (Allen et al. 1998) using the daily weather data. The estimated ET_0 was then multiplied by a crop coefficient (K_c) to estimate onion evapotranspiration (ET_c). K_c values for onion were estimated using the following equation developed by Al-Jamal et al. (1999):

$$K_c = 0.522 - 6.48 \times 10^{-4} \times \mathrm{GDD}_i + 1.98 \times 10^{-6} \times \mathrm{GDD}_i^2 - 8.75 \times 10^{-10} \times \mathrm{GDD}_i^3 \quad (8)$$

$$\mathrm{GDD}_i = T_{\mathrm{avg}} - T_b \quad (9)$$

where GDD_i = growing degree days for day i ($T_{\mathrm{avg}} > T_b$, else GDD = 0) (°C day); T_{avg} = average of daily maximum and minimum air temperatures (°C); and T_b = crop-specific base air

temperature of 4°C for onion (Al-Jamal et al. 1999). When the soil surface was wet following irrigation or rainfall and during early periods after irrigation, E_p was estimated according to Snyder et al. (2000), and T_p was then obtained by subtracting E_p from ET_c. Deb et al. (2011) found that during dry soil conditions, the contribution of the total upward water vapor flux to the total water flux near the soil surface at this onion field was approximately 10%. Therefore, ET_c was partitioned into E_p ($= 0.10ET_c$) and T_p ($= 0.90ET_c$) under dry soil conditions. ET_c, E_p, and T_p during the growing period, used as boundary conditions at the soil surface in the *HYDRUS* model, are shown in Fig. 2.

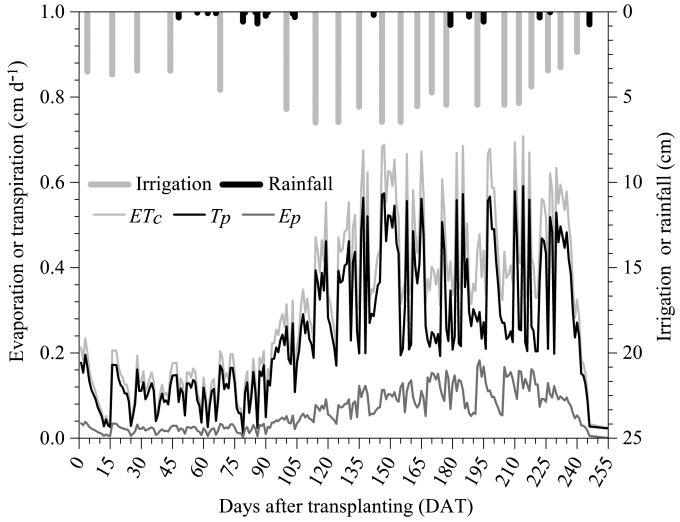

Fig. 2. Potential evapotranspiration (ET_c), soil evaporation (E_p), and transpiration (T_p) during the onion growing season, which were used as boundary conditions at the soil surface (Fig. 1) in *HYDRUS (2D/3D)* simulations

In *HYDRUS*, the spatial distribution of roots is constant in time and their dynamics cannot be considered. As root distribution differs within the growing season, the onion growing season was split into four growth stages: (1) the establishment stage of onion growth (1–90 DAT); (2) development (vegetative) and early stage of bulb formation (91–166 DAT); (3) bulb formation or bulb growth stage (167–207 DAT); and (4) bulb enlargement or maturity stage (208–255 DAT). Water flow and transport of urea, NH_4^+, and NO_3^- was simulated during each of the four growth stages separately. Final volumetric water content, urea, NH_4^+, and NO_3^- distributions in the flow domain (Fig. 1) from the earlier growth stage were used as initial conditions for the subsequent stage.

Onions were transplanted in two rows on each ridge. Onion has a shallow rooting depth (<50 cm) (Al-Jamal et al. 1997; Sharma et al. 2012a, b). Therefore, during each of the four growth stages of onion, rooting depths and root distributions were observed by excavating a soil pit to a soil depth of 80 cm. Soil cores below the furrow (i.e., both the bottom and side of the furrow) and the ridge were collected at 10-cm depth increments down to a depth of 80 cm. Collected soils were washed to extract roots, which were then scanned. An analysis of scanned root images for the root size distribution and the root length density was performed. The majority of the roots were found below the ridge and sloping side of the furrow, and in particular, within the 0–10 cm soil depths during the establishment stage, and within the 0–30 cm soil depths during the development (vegetative) and early stage of bulb formation, bulb formation or bulb growth, and bulb enlargement or maturity stages. Except for the establishment stage when the maximum rooting depth was 30 cm, the maximum rooting depth of 50 cm during the other three growth stages was observed.

In *HYDRUS*, root water uptake reductions attributable to the water stress were described using the piece-wise linear model

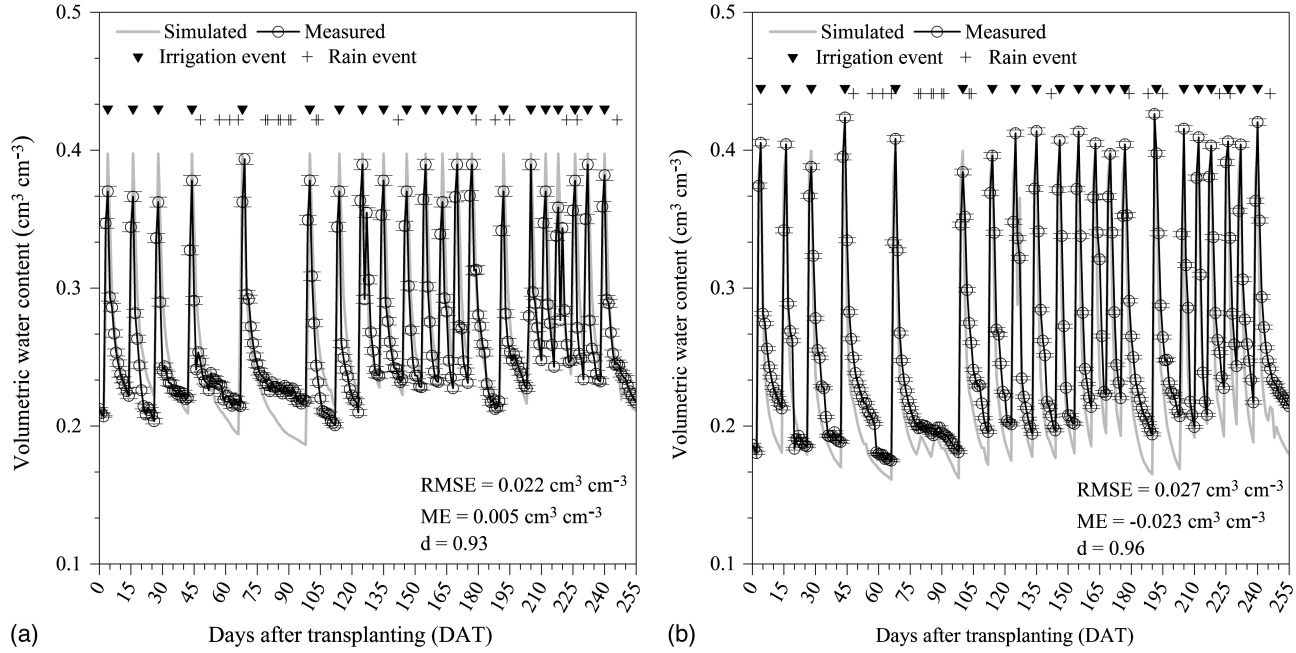

Fig. 3. Comparisons between the measured and simulated daily mean volumetric water contents below the bottom of the furrow at soil depths of: (a) 20 cm; (b) 50 cm during the onion growing season; error bars of the measured values are standard errors of the means; RMSE, ME, and d are the root mean square error, mean bias error, and index of agreement [Eqs. (10)–(12)], respectively, between the measured and simulated volumetric water contents

proposed by Feddes et al. (1978), which includes five variables that describe the dependence of the extraction of water from the soil on ψ. All critical ψ values for the functional form of Feddes et al. (1978) [i.e., ψ_1 (oxygen deficiency point) = $-10, \psi_2 = -25$, $\psi_{3,\text{high}} = -450, \psi_{3,\text{low}} = -550$, and $\psi_4 = -8{,}000$ cm for the establishment stage, and $\psi_1 = -10, \psi_2 = -25$, $\psi_{3,\text{high}} = -550$, $\psi_{3,\text{low}} = -650$, and $\psi_4 = -8{,}000$ cm for the remaining growth stages] were taken from the *HYDRUS* database (Taylor and Ashcroft 1972). Water uptake above ψ_1 and below ψ_4 is assumed to be zero. Water uptake is maximal between ψ_2 and ψ_3 (reduction point). Between ψ_1 and ψ_2 and between ψ_3 and ψ_4, a linear variation is assumed. The value of ψ_3 depends on the water demand of the atmosphere, and the true ψ_3 is interpolated from low ($\psi_{3,\text{low}}$) and high ($\psi_{3,\text{high}}$) values of ψ_3 and T_p.

HYDRUS evaluation was carried out by comparing field measured volumetric water contents (θ) with model simulations using the quantitative measures of model uncertainty reported in Deb et al. (2013), such as the root mean square error (RMSE), the mean bias error (ME), and an index of agreement (d), which are defined as

$$\text{RMSE} = \sqrt{\frac{\sum_{i=1}^{N}(S_i - M_i)^2}{N}} \tag{10}$$

$$\text{ME} = \frac{\sum_{i=1}^{N}(S_i - M_i)}{N} \tag{11}$$

$$d = 1.0 - \frac{\sum_{i=1}^{N}(S_i - M_i)^2}{\sum_{i=1}^{N}(|S_i - M_{\text{avg}}| + |M_i - M_{\text{avg}}|)^2} \tag{12}$$

where N = number of paired measured and simulated values; S_i = ith simulated value; M_i = ith measured value; and M_{avg} = average of measured values. The value of RMSE reflects a magnitude of the mean difference between measured and simulated results. The value of ME indicates a systematic error or bias in the model prediction, i.e., positive and negative values of ME indicate a tendency for an over-prediction or under-prediction, respectively. The index of agreement (d) is not sensitive to systematic model over- or under-prediction (Krause et al. 2005). The d value ranges

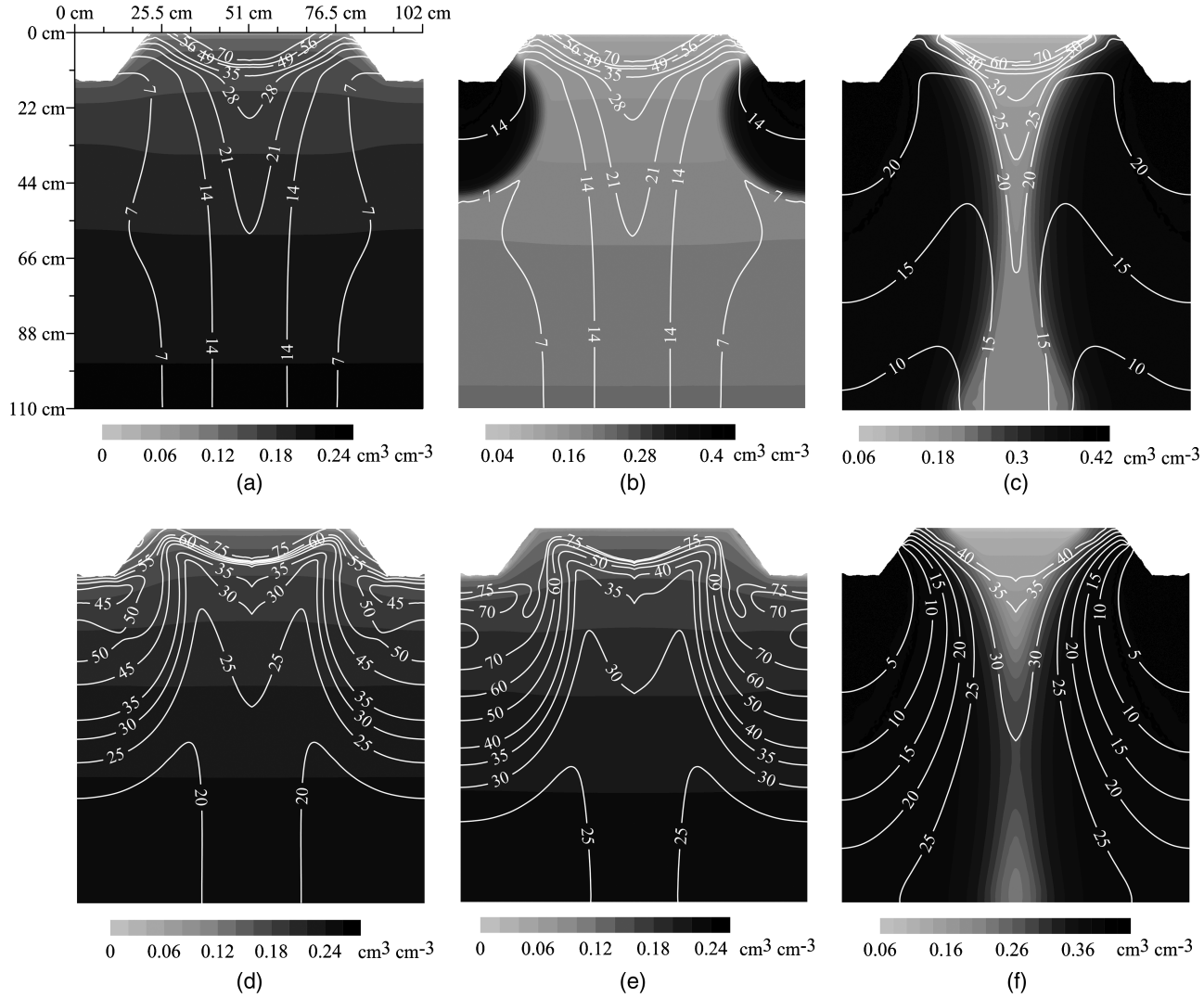

Fig. 4. Simulated spatial distributions of volumetric water contents ($\text{cm}^3\,\text{cm}^{-3}$) (displayed using color maps) and nitrate-nitrogen (NO_3-N) concentrations ($\text{mg}\,\text{L}^{-1}$) (displayed using contour lines with labels) at selected times before and after a furrow fertigation event during the development (vegetative) and early stage of bulb formation: (a) on 145 DAT (days after transplanting), 1 day before the fertigation event; (b) during the fertigation event on 146 DAT; (c) early periods after (i.e., 6 h) the fertigation; (d) on 151 DAT, 5 days after the fertigation; (e) on 154 DAT, 8 days after the fertigation; (f) on 157 DAT, 2 days after the successive irrigation (without fertilizer) event on 155 DAT

between 0 (i.e., no agreement) and 1 (i.e., a perfect fit between simulated and measured values).

Results and Discussion

HYDRUS-simulated and measured volumetric water contents (θ) below the bottom of the furrow at soil depths of 20 and 50 cm are presented in Fig. 3. *HYDRUS* predicted both sharp increases in the volumetric water content following irrigations and then gradual decreases after irrigations. However, the ME value indicated that the model slightly overpredicted θ values at a depth of 20 cm [Fig. 3(a)]. The model predicted slightly higher peak values of θ following irrigations. The model underpredicted θ at 50 cm depth, and the predicted drainage curves were always slightly below the measured curves [Fig. 3(b)]. A comparison between the measured and simulated θ values yielded relatively lower RMSE of 0.022 $cm^3\,cm^{-3}$ and higher d of 0.96 at soil depths of 20 and 50 cm, respectively (Fig. 3). Small differences between the measured and simulated θ values may be partially attributed to measurement errors, which are inevitable under field conditions (Deb et al. 2011, 2013).

Overall, statistics of RMSE, ME, and the index of agreement (d) for simulated and measured θ values [Eqs. (10)–(12)], presented in Fig. 3, suggest that although *HYDRUS* was not calibrated to optimize water flow parameters there was generally a close agreement between the measured and simulated θ values throughout the growing season. This close agreement was primarily attributable to the fact that the measured θ_r, θ_s, α_v, n, l, and K_s parameters used for the parameterization of the van Genuchten–Mualem constitutive relationships [Eqs. (2)–(3)] were within the range of the a-priori parameter distribution and their optimized values previously reported in a *HYDRUS–1D* model (Šimůnek et al. 2013) validation study in this onion field (Deb et al. 2011). Moreover, similar discrepancies (i.e., RMSE, ME, and d) between the measured and simulated θ values were reported in Deb et al. (2013).

Simulated spatial distributions of volumetric water contents and NO_3-N concentrations, and changes in volumetric water contents and NO_3-N profiles at selected times before and after the fertigation event (at a rate of 49.2 kg N ha^{-1} per irrigation; Table 1) on 146 DAT are displayed in Fig. 4. On 145 DAT [1 day before the fertigation event; Fig. 4(a)], NO_3-N concentrations remained much higher within the upper 0 to 15 cm soil depths below the ridge and side of the furrow.

The relatively high NO_3-N concentration near the ridge reflected the distribution of NO_3-N accumulated with time from the previous fertigation on 125 DAT (Table 1), suggesting that supply of NO_3-N by the UAN fertilizer and nitrification of NH_4^+ exceeded the NO_3-N removal by root uptake (discussed later). As shown in Figs. 4(b and c), NO_3-N increased below the bottom of the furrow and moved laterally and vertically as a result of the fertigation. 5 to 8 days after the fertigation event [Figs. 4(d and e)],

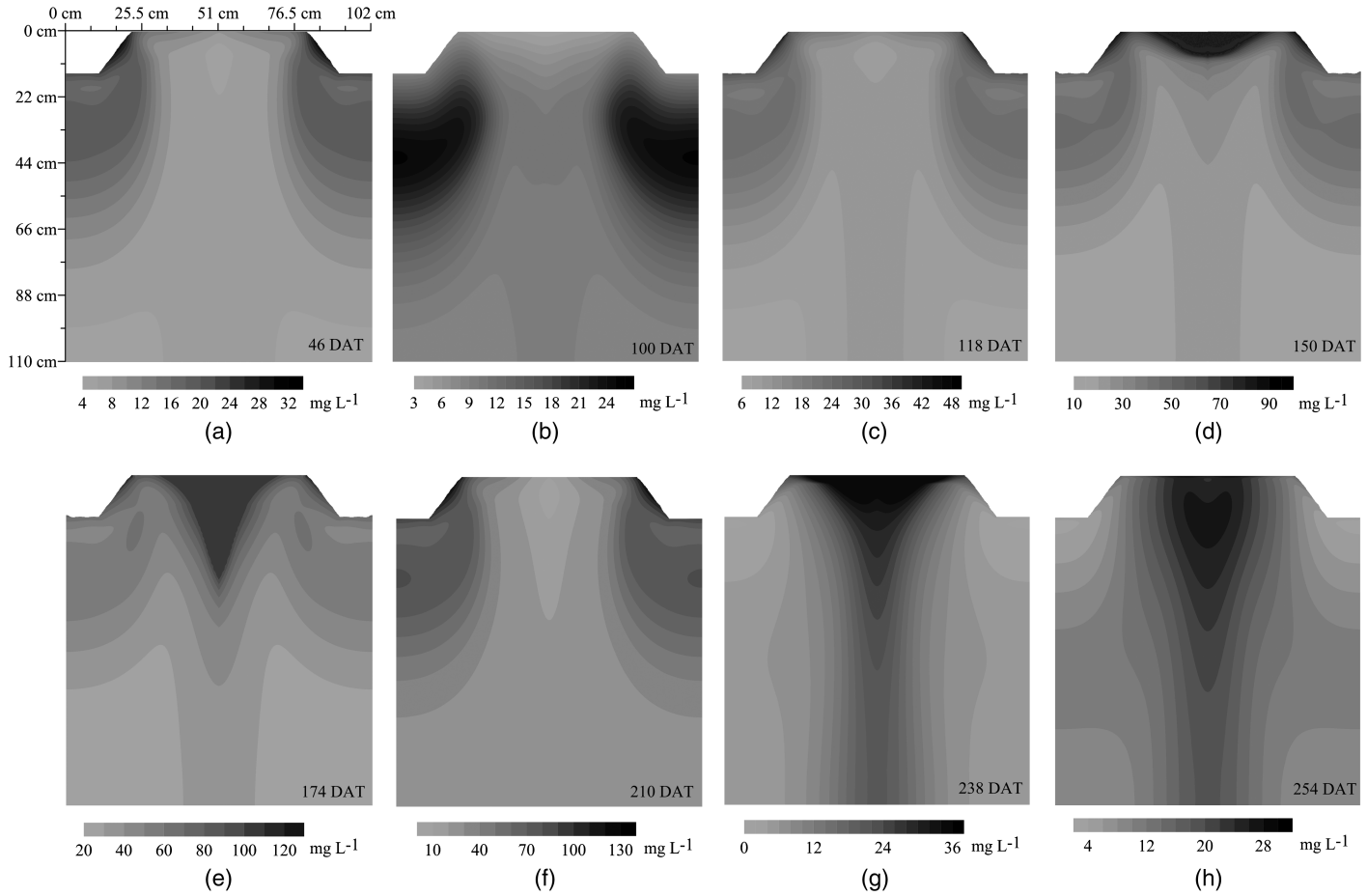

Fig. 5. Simulated spatial distributions of nitrate-nitrogen (NO_3-N) concentrations within the flow domain at different times during the onion growing season: (a and b) on 46 DAT (days after transplanting) and 100 DAT of the establishment stage of onion growth; (c and d) on 118 DAT and 150 DAT of the development (vegetative) and early stage of bulb formation; (e) on 174 DAT of the bulb formation and bulb growth stage; (f and g) on 210 DAT and 238 DAT of the bulb enlargement or maturity stage; (h) on 254 DAT prior to the harvest on 255 DAT

NO_3-N concentrations below the ridge and the furrow (both the bottom and side of the furrow) remained much higher within the root zone (0 to 50 cm soil depths), and in particular, within the upper 0–30 cm depths, where the majority of roots were observed.

On 157 DAT [i.e., 2 days after the successive irrigation event without a fertilizer application; Fig. 4(f)], NO_3-N concentrations decreased within the 0–50 cm depths of the flow domain. As shown in Fig. 4(f), spatial distributions of higher NO_3-N concentrations immediately below and within the ridge and of lower concentrations directly below the bottom of the furrow suggest the dominant effect of the downward movement of irrigation water below the furrow, which is the driving force moving NO_3-N out of the soil below the furrow. Therefore, the zone of the maximum NO_3-N concentrations remained at a depth of 0–30 cm below the ridge and side of the furrow, enabling its continued uptake by onions. However, NO_3-N concentrations gradually increased in deeper depths (below 30 cm) with time after a fertigation event [Figs. 4(a–e)]. NO_3-N, which is only weakly adsorbed to the soil particles (unlike NH_4^+) (González-Delgado and Shukla 2014) and has high mobility, was transported with irrigation water. Because the majority of roots were within the upper 0–30 cm depths during this development (vegetative) and early stage of bulb formation, NO_3-N below the 50 cm soil depth (i.e., the maximum rooting depth observed at this growth stage) was not available for uptake by onions, leading to eventual leaching losses.

In general, NO_3-N concentrations increased with time during the soil drying period after the fertigation event [Figs. 4(d and e)], particularly within the upper 30 cm soil depth below the ridge and the furrow. The increase in NO_3-N concentrations with increasing soil drying can be explained by NH_4^+ nitrification in the soil as nitrification only occurs under aerobic conditions (Rodríguez et al. 2005). This also suggests that nitrification under the furrow fertigation with the urea-ammonium-nitrate (UAN) liquid fertilizer is particularly important near the soil surface at the ridge and the furrow. In a *HYDRUS–2D* simulation, although reported for the drip fertigation, Hanson et al. (2006) also found that NO_3^- concentrations throughout the soil profile increased with time, particularly near the soil surface, because of the hydrolysis and nitrification of the applied urea-ammonium-nitrate fertilizer, in contrast to the study that used nitrate-only fertilizer (Gärdenäs et al. 2005).

Spatial distributions of simulated NO_3-N concentrations in the flow domain at different times are shown in Fig. 5. Note that monthly field observations of NO_3-N concentrations within the 0 to 110 cm soil depths during the growing season were also made at the same times. Higher NO_3-N concentrations were found in the root zone (above the 50 cm soil depth) than below the root zone

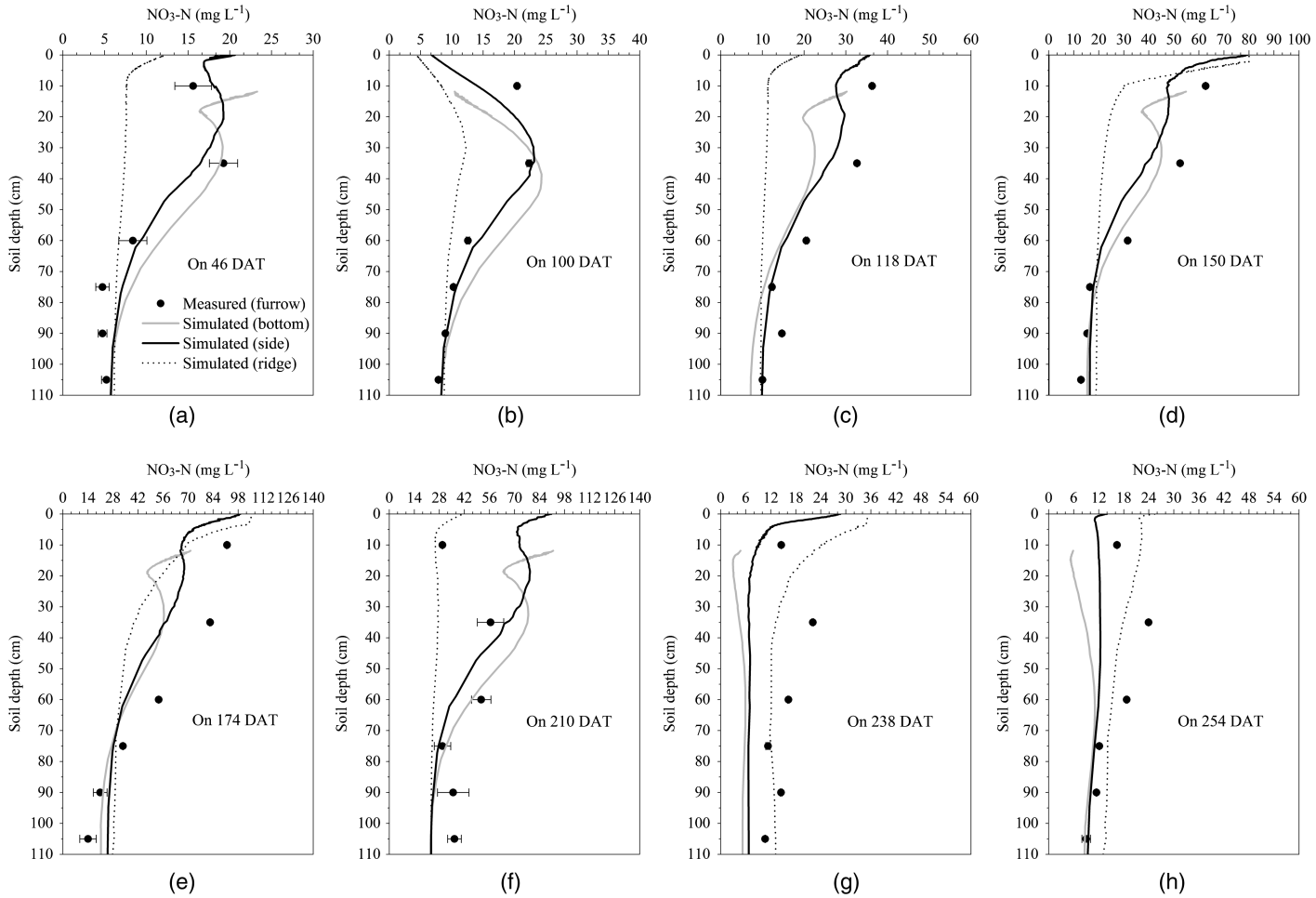

Fig. 6. Simulated nitrate-nitrogen (NO_3-N) concentration profiles at the bottom and sloping side of the furrow (at a distance of 12 and 22 cm from the point *A*, respectively; Fig. 1), at the ridge (at 36 cm from A; Fig. 1), and measured NO_3-N concentration profiles at the furrow at different times during the onion growing season: (a and b) on 46 DAT (days after transplanting) and 100 DAT of the establishment stage of onion growth; (c and d) on 118 DAT and 150 DAT of the development (vegetative) and early stage of bulb formation; (e) on 174 DAT of the bulb formation or bulb growth stage; (f and g) on 210 DAT and 238 DAT of the bulb enlargement or maturity stage; (h) on 254 DAT prior to the harvest on 255 DAT; error bars of the measured values are standard errors of the means

during all four growth stages of onion. NO_3-N concentrations within the root zone also remained much higher even after an irrigation (without fertilizer) event. For example, after the fertigation event on 28 DAT (Table 1), higher NO_3-N concentration was observed below the furrow on 46 DAT [Fig. 5(a)], even after the irrigation (without fertilizer) event on 44 DAT (Table 1). However, as shown in Figs. 5(c–h), NO_3-N concentrations below the root zone (below 50 cm) were much higher than the U.S. Environmental Protection Agency's drinking water standard of 10 mg L^{-1} (U.S. EPA 2012). The observation of higher NO_3-N concentrations below the root zone was in agreement with other studies that were carried out on a furrow-irrigated onion field in semiarid southern New Mexico [e.g., Sharma et al. (2012b)].

Fig. 6 compares simulated depth distributions of NO_3-N concentrations at locations in the furrow (both at the bottom and side of the furrow) and at the ridge with the measured NO_3-N concentration profiles observed in the furrow during the growing season. Changes in the measured mean NO_3-N concentration profiles at selected times were compared with the simulated ones at locations in the furrow and at the ridge (Fig. 6) to understand the NO_3-N distribution and redistribution processes following irrigation and fertigation. *HYDRUS* simulations produced similar patterns of NO_3-N concentration profiles as those measured, with the NO_3-N concentrations remaining higher in the root zone throughout the growing season [Figs. 6(a–h)].

Overall, measured depth distributions of NO_3-N concentrations at different times during different growth stages of onion were comparable with the simulated NO_3-N concentration profiles at the furrow and at the ridge [Figs. 6(a–h)]. Agreement between the measured and simulated depth distributions of NO_3-N concentrations was less satisfactory only for measurements on 238 DAT and 254 DAT, as shown in Figs. 6(g and h), respectively. Differences were likely caused by the solute transport parameters such as K_d, μ_a, and μ_n in the model parameterization, which were taken from the literature and were not optimized for these particular conditions. Differences might also relate in part to measurement errors, particularly on 238 DAT and 254 DAT. It is worth noting that, as reported in other studies, even a calibrated model could produce poor agreement between the measured and simulated depth distributions of solute concentrations below the furrows because of the substantial spatial and temporal variations in solute transport parameters [e.g., Abbasi et al. (2004)].

Simulated cumulative total actual evaporation and transpiration, and cumulative amount of NO_3-N removed from the flow domain by root water uptake during the four growth stages of onion are shown in Figs. 7(a–d). Root nutrient uptake was simulated assuming that all uptakes [i.e., last term in Eqs. (4)–(6)] were passive, through the root water uptake pathway only. Therefore, the increase in actual transpiration (i.e., root water uptake) generally resulted in an increase in root NO_3-N uptake [Figs. 7(a–d)]. Simulated cumulative bottom boundary water and NO_3-N fluxes during the four growth stages are presented in Figs. 8(a–d). Higher NO_3-N concentrations, simulated by the *HYDRUS* within the root zone [Figs. 5(a–h) and 6(a–h)], were dependent on fertigation rates (Table 1), NO_3-N uptake by onions [Figs. 7(a–d)], and NO_3-N leaching below the root zone [Figs. 8(a–d)].

During the development (vegetative) and early stage of bulb formation (91–166 DAT), and during the bulb formation or bulb

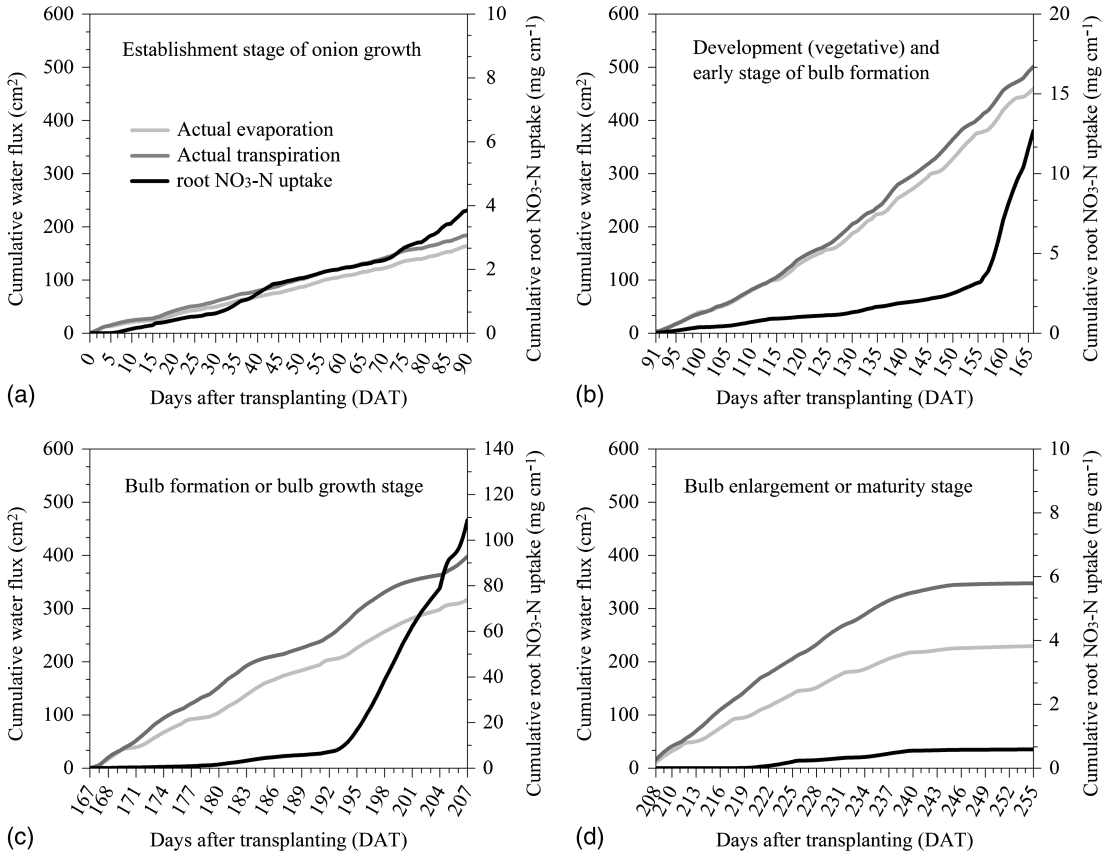

Fig. 7. Simulated cumulative total water fluxes (total actual evaporation and transpiration rates) (cm^2) and cumulative amount of nitrate-nitrogen (NO_3-N) (mg cm^{-1}) removed from the flow region by root uptake during: (a) the establishment stage of onion growth; (b) the development (vegetative) and early stage of bulb formation; (c) the bulb formation or bulb growth stage; (d) the bulb enlargement or maturity stage

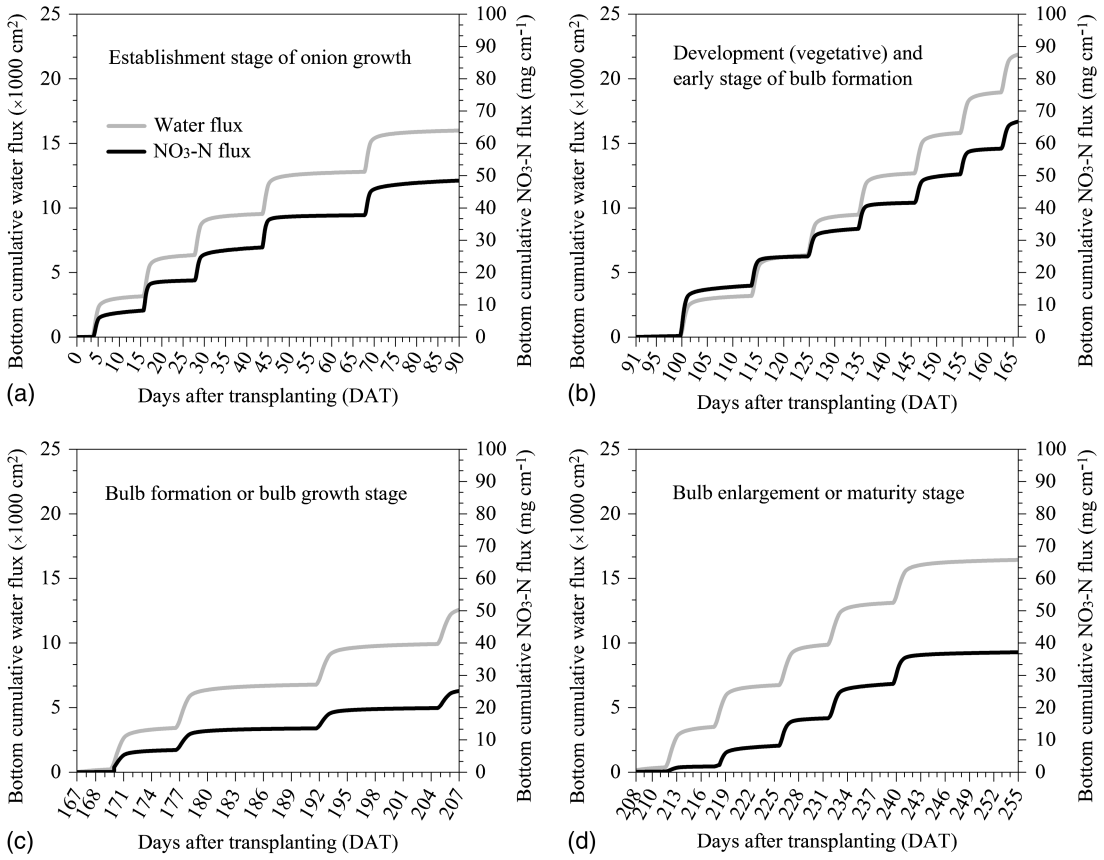

Fig. 8. Simulated cumulative bottom boundary water (×1,000 cm^2) and nitrate-nitrogen (NO_3-N) (mg cm^{-1}) fluxes during: (a) the establishment stage of onion growth; (b) the development (vegetative) and early stage of bulb formation; (c) the bulb formation or bulb growth stage; (d) the bulb enlargement or maturity stage

growth stage (167–207 DAT), the accumulation of higher NO_3-N concentrations simulated by the *HYDRUS* below the furrow bottom and the ridge on 150 DAT [Figs. 5(d) and 6(d)] and 174 DAT [Figs. 5(e) and 6(e)] suggested that the supply of NO_3-N by the UAN fertilizer exceeded the NO_3-N removal by root uptake [Figs. 7(b and c)], respectively). It is worth noting that whereas the root NO_3-N uptake likely involves both passive and active mechanisms [e.g., Šimůnek and Hopmans (2009)], considering only passive NO_3-N uptake might underestimate the simulated total NO_3-N uptake [Figs. 7(b and c)] and overestimate downward NO_3-N leaching on 150 DAT and 174 DAT [Figs. 8(b and c)]. The accumulation of higher NO_3-N concentrations within the root zone [Figs. 5(f) and 6(f)], but markedly lower NO_3-N removal by root uptake [Fig. 7(d)] and lower NO_3-N leaching [Fig. 8(d)] were observed on 210 DAT.

Similar to measurements, simulated NO_3-N concentrations gradually decreased during different growth stages of onion (155–255 DAT), particularly from the early stage of bulb formation through the bulb enlargement or maturity stage [e.g., Figs. 5(f–h) and 6(f–h)], primarily because of higher NO_3-N uptake [Figs. 7(b–d)]. Several studies reported that onion crops need a maximum amount of N during the bulb formation and bulb growth stage [e.g., Halvorson et al. (2002) and Sharma et al. (2012b)]. Simulations of NO_3-N distributions indicated that most fertigation events could be applied at an early stage of bulb formation to supply the maximum NO_3-N demands of onions. This would also reduce the NO_3-N leaching that occurred during other period, particularly between the establishment stage and an early stage of development (or vegetative growth) [Figs. 8(a and b)]. However, there is a need to extend this numerical modeling study over multiple growing seasons to assess total NO_3-N uptake by onion and NO_3-N leaching under conventional furrow fertigation with the UAN fertilizer.

HYDRUS simulations also quantified the distributions of urea and ammonium-nitrogen (NH_4-N) [i.e., $0.78 \times NH_4^+$ (mg L^{-1})] within and below the crop zone. However, because urea and NH_4-N concentrations were not measured in the field, focus here is only on spatial and temporal distributions of NO_3-N within and below the onion root zone. Further investigation into *HYDRUS*'s ability, particularly a field validation, to adequately quantify distributions of all N species (urea, NH_4-N, and NO_3-N) within and below the onion root zone under a conventional furrow fertigation with the UAN fertilizer is suggested.

Summary and Conclusions

The *HYDRUS* model was used as a tool to simulate water flow and NO_3-N transport in the onion root zone for furrow fertigation with the UAN fertilizer. *HYDRUS*-simulated volumetric water contents agreed well with the measurements. Simulations produced similar patterns of monthly measured NO_3-N concentration profiles. Overall, measured depth distributions of NO_3-N concentrations within and below the root zone during different growth stages of onion were comparable with the simulated NO_3-N concentration profiles. During the growing season, NO_3-N concentrations were generally higher within the root zone (50 cm soil depth from the ridge). Accumulation of NO_3-N was also observed within this soil depth.

Higher NO_3-N concentrations were dependent on the rate of the UAN fertilizer application, quantity of NO_3-N removed from the root zone region by root uptake, and NO_3-N leaching below the root zone. Simulations also suggested that NO_3-N below the root zone (below 50 cm soil depth) during different growth stages remained much higher than a recommended standard for the NO_3-N concentration level of 10 mg L^{-1} (for drinking water). This resulted in higher NO_3-N drainage fluxes, particularly during the period between the establishment and vegetative growth stages and thus, warrants the need to apply most fertigation events at an early stage of bulb formation to increase NO_3-N uptake and reduce NO_3-N leaching. Further field validation of the *HYDRUS* aimed at examining distributions of all N species (urea, NH_4-N and NO_3-N) within and below the onion root zone under a conventional furrow fertigation with the UAN fertilizer is suggested.

Acknowledgments

The authors thank New Mexico State University Agricultural Experiment Station for funding this research.

References

Abbasi, F., Feyen, J., and van Genuchten, M. Th. (2004). "Two-dimensional simulation of water flow and solute transport below furrows: Model calibration and validation." *J. Hydrol.*, 290(1–2), 63–79.

Al-Jamal, M. S., Sammis, T. W., Ball, S., and Smeal, D. (1999). "Yield based, irrigated onion crop coefficients." *Appl. Eng. Agric.*, 15(6), 659–668.

Al-Jamal, M. S., Sammis, T. W., and Jones, T. (1997). "Nitrogen and chloride concentration in deep soil cores related to fertilization." *Agric. Water Manage.*, 34(1), 1–16.

Allen, R. G., Pereira, L. S., Raes, D., and Smith, M. (1998). "Crop evapotranspiration: Guidelines for computing crop water requirements." Food and Agriculture Organization of the United Nations, Rome.

Beven, K. J., Henderson, D. E., and Reeves, A. D. (1993). "Dispersion parameters for undisturbed partially saturated soil." *J. Hydrol.*, 143(1–2), 19–43.

Böhlke, J.-K. (2002). "Groundwater recharge and agricultural contamination." *Hydrogeol. J.*, 10(1), 153–179.

Cote, C. M., Bristow, K. L., Charlesworth, P. B., Cook, F. J., and Thorburn, P. J. (2003). "Analysis of soil wetting and solute transport in subsurface trickle irrigation." *Irrig. Sci.*, 22(3–4), 143–156.

Crevoisier, D., Popova, Z., Mailhol, J. C., and Ruelle, P. (2008). "Assessment and simulation of water and nitrogen transfer under furrow irrigation." *Agric. Wat. Manage.*, 95(4), 354–366.

Deb, S. K., Shukla, M. K., Sharma, P., and Mexal, J. G. (2011). "Coupled liquid water, water vapor, and heat transport simulations in an unsaturated zone of a sandy loam field." *Soil Sci.*, 176(8), 387–398.

Deb, S. K., Shukla, M. K., Šimůnek, J., and Mexal, J. G. (2013). "Evaluation of spatial and temporal root water uptake patterns of a flood-Irrigated pecan tree using the HYDRUS (2D/3D)." *J. Irrig. Drain. Eng.*, 10.1061/(ASCE)IR.1943-4774.0000611, 599–611.

Feddes, R. A., Kowalik, P. J., and Zaradny, H. (1978). *Simulation of field water use and crop yield*, Wiley, New York.

Gärdenäs, A. I., Hopmans, J. W., Hanson, B. R., and Šimůnek, J. (2005). "Two-dimensional modelling of nitrate leaching for various fertigation scenarios under micro-irrigation." *Agric. Water Manage.*, 74(3), 219–242.

Gile, L. H., Hawley, J. W., and Grossman, R. B. (1981). "Soils and geomorphology in the basin and range area of southern New Mexico: Guidebook to the desert project." New Mexico Bureau of Mines and Mineral Resources, Socorro, NM.

González-Delgado, A. M., and Shukla, M. K. (2014). "Transport of nitrate and chloride in variably saturated porous media." *J. Irrig. Drain. Eng.*, 10.1061/(ASCE)IR.1943-4774.0000725, 04014006-1–04014006-9.

Halvorson, A. D., Follett, R. F., Bartolo, M. E., and Schweissing, F. C. (2002). "Nitrogen fertilizer use efficiency of furrow irrigated onion and corn." *Agron. J.*, 94(3), 442–449.

Hanson, B. R., Šimůnek, J., and Hopmans, J. W. (2006). "Evaluation of urea–ammonium–nitrate fertigation with drip irrigation using numerical modeling." *Agric. Wat. Manage.*, 86(1–2), 102–113.

Krause, P., Boyle, D. P., and Bäse, F. (2005). "Comparison of different efficiency criteria for hydrological model assessment." *Adv. Geosci.*, 5, 89–97.

Ling, G., and El-Kadi, A. I. (1998). "A lumped parameter model for nitrogen transformation in the unsaturated zone." *Water Resour. Res.*, 34(2), 203–212.

Maynard, D. G., and Kalra, Y. P. (1993). "Nitrate and exchangeable ammonium nitrogen." Chapter 4, *Soil sampling and methods of analysis*, M. R. Carter, ed., Canadian Society of Soil Science, Lewis Publishers, Boca Raton, FL, 25–38.

Mualem, Y. (1976). "A new model for predicting the hydraulic conductivity of unsaturated porous media." *Water Resour. Res.*, 12(3), 513–522.

Peterson, G. A., and Power, J. F. (1991). "Soil, crop, and water management." Chapter 9, *Managing nitrogen for groundwater quality and farm profitability*, R. F. Follett, D. R. Keeney, and R. M. Cruse, eds., Soil Science Society of America, Madison, WI, 189–198.

Rodríguez, S. B., Alonso-Gaite, A., and Álvarez-Benedí, J. (2005). "Characterization of nitrogen transformations, sorption and volatilization processes in urea fertilized soils." *Vadose Zone J.*, 4(2), 329–336.

Šejna, M., Šimůnek, J., and van Genuchten, M. Th. (2013). "The HYDRUS software package for simulating the two– and three–dimensional movement of water, heat, and multiple solutes in variably–saturated media." PC–Progress, Prague, Czech Republic.

Sharma, P., Shukla, M. K., Sammis, T. W., and Adhikari, P. (2012a). "Nitrate–Nitrogen leaching from onion bed under furrow and drip irrigation systems." *Appl. Enviorn. Soil Sci.*, 2012, 1–17.

Sharma, P., Shukla, M. K., Sammis, T. W., Steiner, R. L., and Mexal, J. G. (2012b). "Nitrate-nitrogen leaching from three specialty crops of New Mexico under furrow irrigation system." *Agric. Water Manage.*, 109(2012), 71–80.

Šimůnek, J., and Hopmans, J. W. (2009). "Modeling compensated root water and nutrient uptake." *Ecolog. Model.*, 220(4), 505–521.

Šimůnek, J., Šejna, M., Saito, H., Sakai, M., and van Genuchten, M. Th. (2013). "The HYDRUS–1D software package for simulating the one–dimensional movement of water, heat, and multiple solutes in variably–saturated media." *Version 4.16*, Dept. of Environmental Sciences, Univ. of California Riverside, Riverside, CA.

Šimůnek, J., van Genuchten, M. Th., and Šejna, M. (2012). "The HYDRUS software package for simulating the two– and three–dimensional movement of water, heat, and multiple solutes in variably–saturated media." PC–Progress, Prague, Czech Republic.

Siyal, A. A., Bristow, K. L., and Šimůnek, J. (2012). "Minimizing nitrogen leaching from furrow irrigation through novel fertilizer placement and soil surface management strategies." *Agric. Water Manage.*, 115(2012), 242–251.

Snyder, R. L., Bali, K., Ventura, F., and Gomez-MacPherson, H. (2000). "Estimating evaporation from bare or nearly bare soil." *J. Irrig. Drain. Eng.*, 10.1061/(ASCE)0733-9437(2000)126:6(399), 399–403.

Spalding, R. F., and Exner, M. E. (1993). "Occurrence of nitrate in groundwater: A review." *J. Environ. Qual.*, 22(3), 392–402.

Taylor, S. A., and Ashcroft, G. L. (1972). *Physical edaphology: The physics of irrigated and nonirrigated soils*, Freeman, San Francisco.

USDA (U.S. Department of Agriculture). (2014). "Vegetables 2013 summary (March 2014)." National Agricultural Statistics Service, Washington, DC.

U.S. EPA. (2012). "2012 editions of the drinking water regulations and health advisories." *EPA 822-S-12-001*, Office of Water, Washington, DC.

van der Laan, M., Stirzaker, R. J., Annandale, J. G., Bristow, K. L., and du Preez, C. C. (2010). "Monitoring and modelling draining and resident soil water nitrate concentrations to estimate leaching losses." *Agric. Wat. Manage.*, 97(11), 1779–1786.

van Genuchten, M. Th. (1980). "A closed-form equation for predicting the hydraulic conductivity of unsaturated soils." *Soil Sci. Soc. Am. J.*, 44(5), 892–898.

van Genuchten, M. Th., Leij, F. J., and Yates, S. R. (1991). "The RETC code for quantifying the hydraulic functions of unsaturated soils, version 1.0." *EPA/600/2–91/065*, U.S. Salinity Laboratory, Riverside, CA.

Weed, D. A. J., and Kanwar, R. S. (1996). "Nitrate and water present in and flowing from root-zone soil." *J. Environ. Qual.*, 25(4), 709–719.